24th IMEKO TC4 International Symposium
22nd International Workshop on ADC and DAC Modelling and Testing
IMEKO TC-4 2020
Palermo, Italy, September 14-16, 2020

Electrical characterization of a monitoring system for precision farming under temperature stress

Lorenzo Ciani, Marcantonio Catelani, Alessandro Bartolini, Giulia Guidi, Gabriele Patrizi

Department of Information Engineering, University of Florence, via di Santa Marta 3, 50139, Florence, Italy

lorenzo.ciani@unifi.it

***Abstract* – Precision farming is based on monitoring environmental conditions and soil parameter to improve productivity, to optimize soil conservation, to save water and to limit plant diseases. Wireless sensor networks are an optimal solution to implement this monitoring process, covering large area and ensuring fault tolerance. Currently, there are no international standards that deal with environmental testing of Wireless Sensor Networks; therefore a customized test plan was developed basing on a step stress test from 20 °C to 80 °C, with 5 °C steps. The objective of the analysis was to investigate the effects of raised temperature on the performances of a self-designed sensor node. A customized measurement set-up is presented in this paper to test electrical and electronic performances of the node under thermal stress.**

Keywords *– Fault Diagnosis, Precision farming, Temperature, Testing, Wireless Sensor Network*

I. INTRODUCTION

In agriculture 4.0, the monitoring of both environmental conditions and soil parameters is extremely important [1]. A typical solution is to use a Wireless Sensor Network (WSN) to monitor the crop. The network has to endure harsh outdoor conditions, facing both hot summers and cold winters. At the same time the network has to guarantee service continuity ensuring accurate and reliable data. In fact, according to [2], the integration of Big Data technologies represents a key factor in agricultural fields improving productivity and soil conservation, saving water and limiting plant diseases. Lindsey et al. [3] highlights that environmental factors such as temperature and humidity have a deeply influence on plant pathogens such as bacteria, fungi, and viruses.

The monitoring of environmental conditions, together with soil parameters, allows to automatize irrigation minimizing the water waste [4]–[6]. Many papers in recent literature deal with the design of innovative wireless network for agricultural applications. For instance, in [7] the design of a low-power sensor node for rice field based on hybrid antenna is presented, while the design of sensor nodes for mesh network in litchi plantation are proposed in [8] to improve the coverage area and the micro-irrigation management efficiency. Al-Turjman [9] summarizes that an optimal sensor node for agricultural applications is composed by a power unit, processing unit, memory unit, sensing unit, and a communication unit. In particular, it proposes to use soil moisture, relative humidity, temperature, and gas sensors.

Another widely investigated aspect is the nodes deployment since it deeply affects connectivity, coverage area and reliability [10]–[12]. For instance, some papers propose new routing strategies to solve routing problems in traditional WSNs [13], [14]. The problem of optimization of power consumption in low-power node design is fully discussed and solved with many different solutions [15]–[18].

As seen above, many papers in recent literature deals with design and development of WSN for precision farming, while the concept of testing the hardware performances in real conditions is not adequately dealt with. The effects of the operating environment on the dynamic metrological performances of WSN are not sufficiently investigated, as well as reliability analysis considering temperature variations are not available. As observed in previous works on similar systems [19]–[22], environmental stresses such as temperature, humidity, vibration and mechanical shocks deeply influence both reliability and metrological performances of low-cost electronic components, leading to loss of calibrations, measurement variability and a significant growth in component failure rate.

Unfortunately, there are no international standards regarding environmental tests of WSN, as well as customized standard concerning electronic component testing for agricultural applications are not available. For these reasons, this paper proposes a customized test plan and test-bed for the performances characterization of a sensor node under temperature stress.

II. SENSOR NODE UNDER TEST

Wireless Mesh Networks (WMNs) are a particular case of WSN that provides an optimal solution to ensure the monitoring of large geographical areas using several near nodes and dynamic routing tables. In this way it is possible to achieve high-frequency transmissions, high bitrate, full scalability and low management cost [23].

A traditional WSN is usually based on single central node (Access Point - AP) directly connected to all other nodes in the network. The peripheral nodes acquire data by means of a set of sensors, while the AP collect and store all the data. The main drawbacks are the limited coverage area and the restricted number of nodes. Quite the opposite, a WMN is a self-organized and self-configured system made up by lots of nodes and a single central node (called root node in the following) that manages the whole network. Every node is able to interact with the nearby nodes, using them to reach the root node trough undirect paths, allowing large-area coverage [24], [25].

The designed network is based on a group of nodes, each one composed by a power supply, the ESP-32 system-on-a-chip microcontroller by "Espressif", some interface boards and a set of sensors, including an air temperature and humidity sensor, a soil temperature transducer, a soil moisture sensor and a solar radiation sensor. Figure 1 shows the block diagram of the developed sensor node. The power supply system is composed by a photovoltaic panel, two Li-ion batteries, a "Batteries Management System" (BMS) and a "Maximum Power Point Tracking" (MPPT). The radio and processing unit is the real core of the node. It is based on a microcontroller, which is mounted on an evaluation board used for software programming by means of a USB-to-UART bridge controllers. The evaluation board also includes pin interface and power supply by means of an AMS1117 LDO.

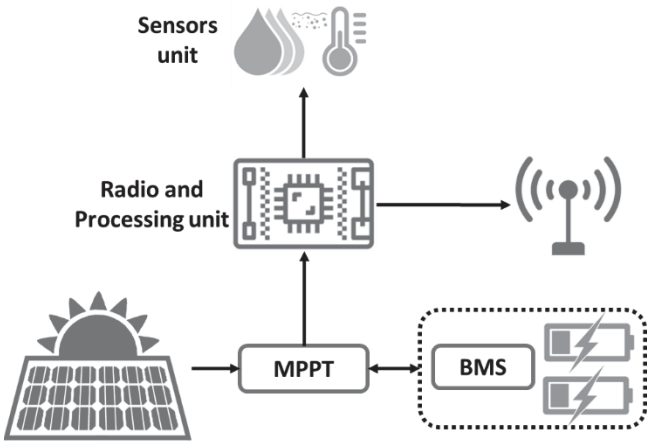

Fig. 1. Block diagram of the sensor node under test, including power management systems, radio and processing unit, external antenna and a set of sensors for environmental monitoring and soil diagnosis.

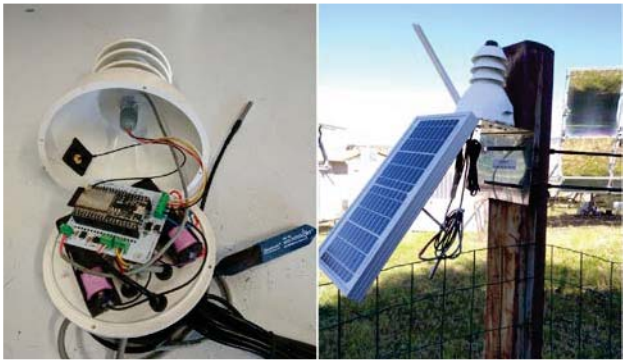

Fig. 2. Images of the developed sensor node. On the lefts side a detail of the boards enclosed inside a waterproof case, while the right image shows the whole node installed on the field (including the photovoltaic panel).

Two 8-channel 12-bit SAR ADCs and two 8-bit DACs are embedded in the ESP-32. A customized interface board is used to connect the batteries, the power boards and the sensors. The network functioning is based on two alternative operating phases: a 10 minutes "sleep phase" in which both hardware and software are disabled to save energy; and a 1 minute "active phase" in which the sensors acquire data, the microcontroller elaborates them and the transceiver transmit information to the root node. This type of functioning minimizes the duty cycle of the network, allowing a reasonable overheating of the network and saving batteries power.

Figure 2 shows two images of the developed sensor node. A detail of the system is illustrated on the left side, while the right image shows the installation on the field.

III. TEMPERATURE STEP-STRESS TEST

In this paper a temperature step-stress test is used to characterize the electrical performances of a sensor node used in precision farming. Temperature has been chosen as stress condition because of the aim of the test, or rather, to characterize the hardware considering the real operating conditions of the node during hot weather summer days. Furthermore, considering the physics of failure, all the typical failure mechanisms of electronic devices are intrinsically related to temperature [26]–[30]. More in detail, failure mechanisms such as open/short circuit, silicon fracture, Electrostatic Discharge (ESD), dielectric charging and many others could be easily triggered by temperature. In other words, temperature is the main accelerating factor of many failure mechanisms of the device under test (DUT). Consequently, it is the optimal stress to characterize both operational performances and reliability at the same time.

The test was developed according to the range of guaranteed operability of both microcontroller and evaluation board which is up to 85 °C. Since international standards devoted to this kind of application are not

available, then the test profile was developed following a set of standards that cover similar area. For instance, the IEC 60068-2-14 (2011) [31] provides general procedures for temperature testing; the IEST-RP-PR-003.1 (2012) [32] defines a temperature step-stress test for accelerating life test; the MIL-STD 810G (2008) [33] is a guideline for any kind of environmental stress tests; the JEDEC JESD22 A104E (2014) [34] covers the temperature test of semiconductor devices.

The profile resembles the ones proposed in the previous standards and is tailored on the practical application scenario. The test starts at 20°C which is generally the room temperature. 10 minutes of exposition time are required to ensure at least one active phase of the node.

The following step consists in a 5 °C raising temperature lasts 10 minutes. The rise speed is intentionally kept low to allow components temperature to increase together with chamber temperature. Then 20 minutes of exposition time at the reached temperature are required to ensure at least two active phases after temperature stability. The two previous steps are repeated up to 80 °C, alternating a 5 °C step (10 minutes) and a 20 minutes exposition time. After reaching 80 °C the temperature is lowered to 20 °C at low rate to ensure gradual cooling of the components.

Fig. 3 shows the trend of the temperature inside the chamber during the test acquired by the PT100 temperature sensor embedded in the climatic chamber. The figure highlights the two different steps of the test: rising time and exposition time.

The complete measurement set-up is illustrated in figure 4. It was composed by a climatic chamber, a datalogger equipped with ten k-type thermocouples, a power supply generator, an oscilloscope, a set of multimeters, a current generator and a waveform generator. Two sensor nodes were located inside the chamber, the first one supplied by the LDO provided by the manufacturer of the evaluation board (AMS1117 LDO - "Former LDO" in the following) and the other one equipped with a AP2114H LDO ("New LDO" in the following). The set-up also included a root node managing the network functionalities and a laptop.

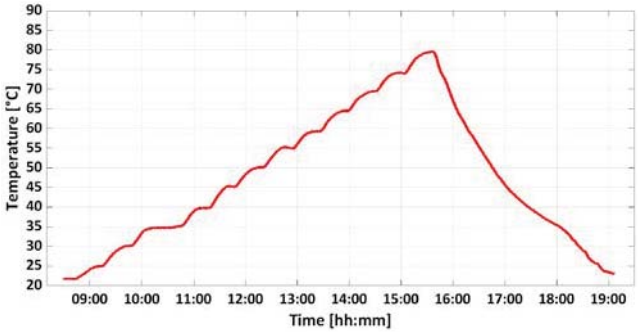

Fig. 3. Step-stress test profile used during the thermal characterization of the sensor node. The trend was acquired by the PT100 temperature sensor of the chamber.

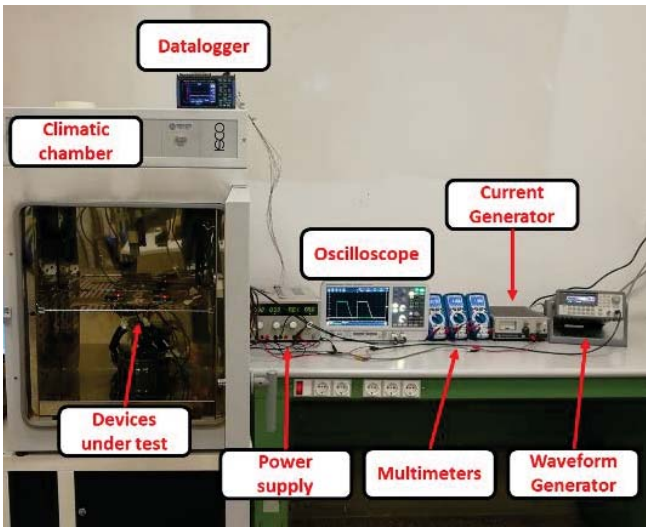

Fig. 4. Measurement set-up developed for the sensor node characterization under temperature stress.

Figure 5 shows a detail of the thermocouples acquisition during the exposition time at 40 °C. Three thermocouples were used to monitor the microcontroller, the LDO and the electronic board of the first node, while other three thermocouples acquire temperature data from the same components of the second node. The temperature spike of some signals observed in the figure has occurred during all the active phases of the node, while during the sleep phases all the temperatures tend to stabilize approximately to the temperature of the chamber. The highest spikes were observed on the temperature of the LDOs (approximately 5 °C higher than the chamber temperature). Microprocessors increase their temperature of approximately 3 °C, while the boards are subjected to 2 °C overheating. Regardless the temperature of the chamber, the observed overheating is approximately the same at each active phase. It could be considered not relevant from a reliability point of view because it is moderate in both amplitude and time duration.

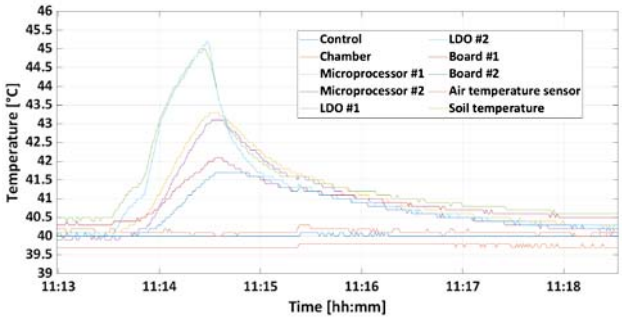

Fig. 5. Detail of the temperature acquired using ten thermocouples and a datalogger. The temperature of the chamber was 40 °C, while the hardware shows a moderate overheating.

IV. CURRENT CONSUMPTION ANALYSIS

Power consumption is an important parameter for stand-alone systems. The board was tested with two different LDOs: the one provided by the manufacturer and a new one. The aim of this procedure is to investigate if the new LDO provides significant upgrades with respect to the former LDO and to evaluate the effect of the temperature, during the step-stress test. Therefore, two multimeters were used to measure the current consumption of the two nodes. Fig. 6 shows the comparison of the two boards' current consumption (blue and green lines) during six cycle of active and sleep phases, with a corresponding chamber temperature from 55 ° C to 65 °C (red line). Moreover, the figure highlights the benefits introduced by the new LDO in both active and sleep phases. In fact, the new LDO allows an average decrease of the absorbed current of 2 mA. Analyzing only one board, there is no variation in the consumption during the active phases in the entire temperature range, regardless the LDO.

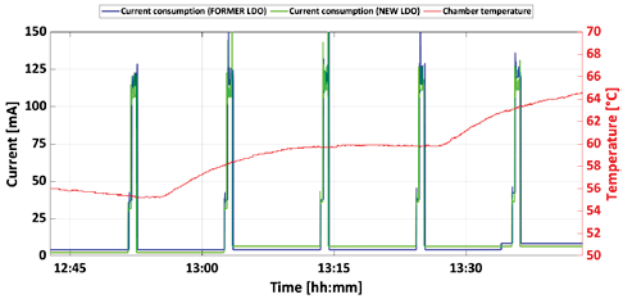

Fig. 6. Current consumption of the two boards (blue and green lines) on the left y-axis while the right y-axis shows the temperature variation of the chamber (red line).

While Fig. 6 highlights the presence of a current step-up for both the sensor nodes during a particular sleep phase. In case of the former LDO the step-up occurs approximately around 63 °C, while the new LDO is subjected to this phenomenon at lower temperature (approximately 58 °C). Indeed, focusing only on the sleep phase, as shown in Fig. 7, it is possible to identify an unexpected increase of about 4.5 mA of the current above a specific temperature in both nodes. During the cooling phase of the chamber the current consumption suddenly decreases assuming the previous value. After a deep analysis, this anomaly is due to an unexpected activation of the USB-to-UART bridge controllers (CP2102N) integrated in the evaluation board. The controller should only be activated (or enabled) in case of a device connection to the USB port as shown in the green box of Fig. 8.

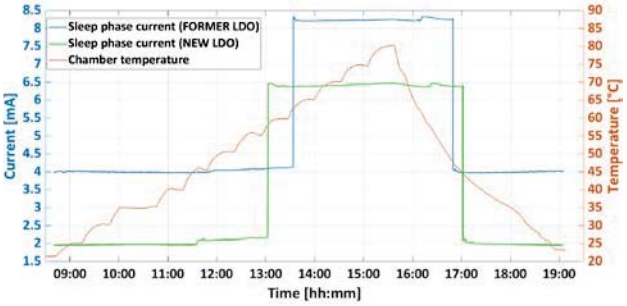

Fig. 7. Detail of the current consumption during the sleep phases of the two boards (blue and green lines) on the left y-axis while the right y-axis shows the temperature variation of the chamber during the test (red line).

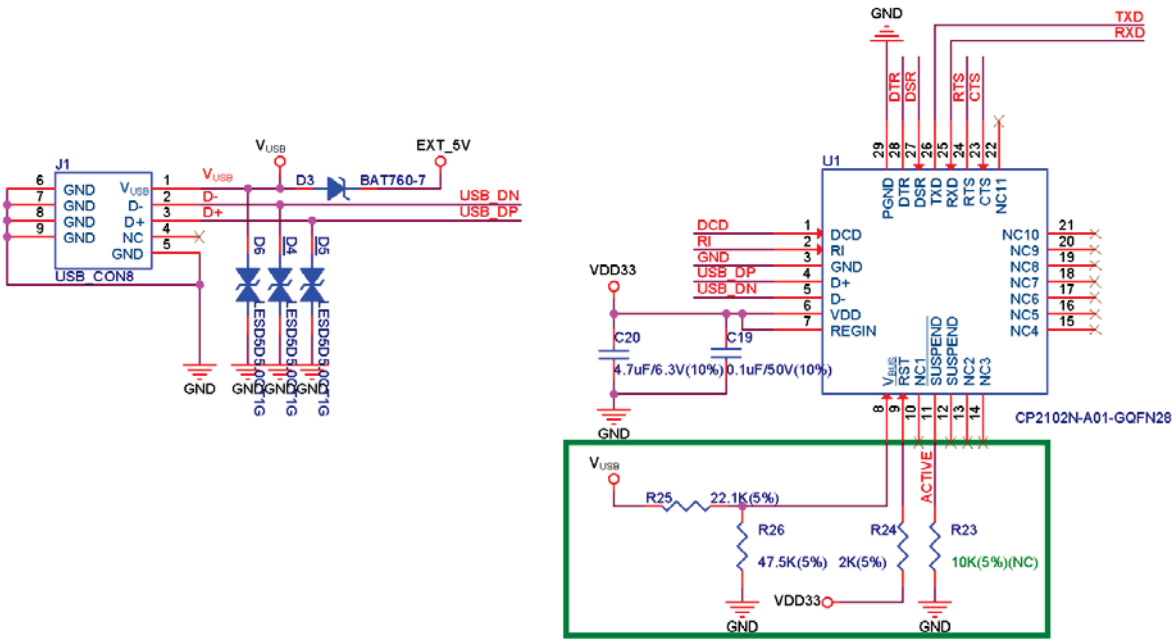

Fig. 8. Schematics of the USB connector and USB-to-UART bridge controllers of ESP32 evaluation board

The 3.3 V output of the LDO supplies both USB-to-UART controller and microcontroller. The CP2102N controller is enabled only in case a USB device is connected to the board (V_{USB}). Under typical operating conditions, the USB provides a 5 V voltage, then the divider R25-R26 generates a voltage drop (V_{BUS}) as input of the 8th pin of the USB-to-UART controller. V_{BUS} can be calculated as follow:

$$V_{BUS} = V_{R26} = \frac{R26}{(R26 + R24)} \cdot V_{USB} = 3.41\,V \qquad (1)$$

The CP2102N datasheet highlights that V_{BUS} pin is considered in a high logical state (controller on) when $V_{BUS} > (VDD - 0.6\,V)$, up to a maximum acceptable value of $VDD + 2.5\,V$. Since VDD=VDD33=3.3 V the high-state threshold can be calculated as:

$$V_{th} = VDD - 0.6 = 3.3 - 0.6 = 2.7\,V \qquad (2)$$

The board is also powered by an external voltage of 5 V (EXT-5V in the schematic in figure 8). The controller is disabled by the Schottky diode (BAT760-7) located between the USB connector and the EXT_5V pin (see the left side of the electronic circuit in Fig 8). This diode allows to do not turn on the USB-to-UART bridge with an external 5V supply. Furthermore it also protects computer or other devices connected via USB from unexpected reverse current. Analyzing the Schottky diode datasheet, it is evident that the increase of temperature produces an increase of the reverse current of the diode. For example, at 75 °C with a 5 V of reverse voltage the diode has a reverse current of about 100 µA.

Since the USB connector is an open circuit and considering negligible the current on the ESD protection diode (D6), the reverse current of the Schottky diode generates a voltage drop on R26 given by:

$$V_{BUS} = V_{R26} \cong 100\,\mu A \cdot 47.5\,k\Omega \qquad (3)$$

$$V_{BUS} = 4.75\,V \gg V_{th} \qquad (4)$$

Therefore, this reverse current evaluated at 75 °C is enough to enable the USB-to-UART controller. Furthermore, this reverse current could be dangerous for higher temperatures because it could generate activation voltages higher than the maximum limit, leading to possible damages of the converter. Consequently, the higher the temperature, the higher the diode reverse current, the higher the activation voltage of the CP2102N controller. If the temperature is higher enough to produce a reverse current which generates a $V_{BUS} > V_{th}$, then the USB-to-UART controller turns on absorbing 4.5 mA and generating the current step shown in the previous figures.

There are two possible corrective actions to delete this problem guaranteeing the proper functionalities in case of a connected USB device:

- change the Schottky diode with another model able to guarantee a lower reverse current;
- modify the R25-R26 divider, for example by maintaining the ratio between the resistances but decreasing the resistance value.

The previous considerations explain also the reason why the current step-ups occurred at different temperature in the boards. Indeed, by measuring the outputs of the two LDOs, it is possible to verify a slight difference in the output voltage that leads to a different voltage threshold (Equation 2) and consequently a different reverse current to activate the USB-to-UART controller.

V. CONCLUSION

The paper deals with the characterization of a sensor node, used in a wireless mesh network, under temperature stress. Since there is not a specific standard for this kind of system, a customized test plan was developed in this work. The system was tested in a climatic chamber under a temperature step profile, starting from 20 °C up to 80 °C (5 °C step), then temperature is lowered to 20 °C at low rate to ensure gradual cooling of the component. The aim of this experiment is to observe the effects of high temperature on the hardware and firmware bugs, looking for any anomalies from the correct functioning. One of the main unexpected finding is an increase of the current consumption during the sleep phase when temperature overpass a certain value. In particular, a 4.5 mA step was verified above a specific temperature. This step is not due to a permanent failure, because during the cooling phase the current returns to its normal value at approximately the same temperature.

This unexpected behavior can lead to an increase of the power consumption of the sensor node and a solution must be considered. The main causes of this anomaly were investigated and after a deep analysis the solutions are proposed. In particular to overcome this problem it is possible to change the Schottky diode with another model able to guarantee a lower reverse current or to modify the divider.

REFERENCES

[1] M. Catelani, L. Ciani, A. Bartolini, G. Guidi, and G. Patrizi, "Standby redundancy for reliability improvement of wireless sensor network," in *5th International Forum on Research and Technologies for Society and Industry*, 2019.

[2] M. Lezoche, J. E. Hernandez, M. del M. E. Alemany Díaz, H. Panetto, and J. Kacprzyk, "Agri-food 4.0: A survey of the supply chains and technologies for the future agriculture," *Comput. Ind.*, vol. 117, p. 103187, May 2020.

[3] A. P. J. Lindsey, S. Murugan, and R. E. Renitta, "Microbial disease management in agriculture: Current status and future prospects," *Biocatal. Agric. Biotechnol.*, vol. 23, p. 101468, Jan. 2020.

[4] H. Zia, N. R. Harris, G. V. Merrett, M. Rivers, and N. Coles, "The impact of agricultural activities on water quality: A case for collaborative catchment-scale management using integrated wireless sensor networks," *Comput. Electron. Agric.*, vol. 96, pp. 126–138, Aug. 2013.

[5] G. Vellidis, M. Tucker, C. Perry, C. Kvien, and C. Bednarz, "A real-time wireless smart sensor array for scheduling irrigation," *Comput. Electron. Agric.*, vol. 61, no. 1, pp. 44–50, Apr. 2008.

[6] J. McCulloch, P. McCarthy, S. M. Guru, W. Peng, D. Hugo, and A. Terhorst, "Wireless sensor network deployment for water use efficiency in irrigation," in *Proceedings of the workshop on Real-world wireless sensor networks - REALWSN '08*, 2008, p. 46.

[7] H. Chen, W. Wang, B. Sun, J. Weng, and F. Tie, "Design of a WSN Node for Rice Field Based on Hybrid Antenna," in *2017 International Conference on Computer Network, Electronic and Automation (ICCNEA)*, 2017, pp. 276–280.

[8] X. Jiaxing, G. Peng, W. Weixing, L. huazhong, X. Xin, and H. Guosheng, "Design of Wireless Sensor Network Bidirectional Nodes for Intelligent Monitoring System of Micro-irrigation in Litchi Orchards," *IFAC-PapersOnLine*, vol. 51, no. 17, pp. 449–454, Jan. 2018.

[9] F. Al-Turjman, "The road towards plant phenotyping via WSNs: An overview," *Comput. Electron. Agric.*, vol. 161, pp. 4–13, Jun. 2019.

[10] M. Younis and K. Akkaya, "Strategies and techniques for node placement in wireless sensor networks: A survey," *Ad Hoc Networks*, vol. 6, no. 4, pp. 621–655, Jun. 2008.

[11] F. M. Al-Turjman, A. E. Al-Fagih, W. M. Alsalih, and H. S. Hassanein, "Reciprocal public sensing for integrated RFID-Sensor Networks," in *2013 9th International Wireless Communications and Mobile Computing Conference (IWCMC)*, 2013, pp. 746–751.

[12] F. M. Al Turjman and H. S. Hassanein, "Towards augmented connectivity with delay constraints in WSN federation," *Int. J. Ad Hoc Ubiquitous Comput.*, vol. 11, no. 2/3, p. 97, 2012.

[13] Y. Wang, X. Li, W.-Z. Song, M. Huang, and T. A. Dahlberg, "Energy-Efficient Localized Routing in Random Multihop Wireless Networks," *IEEE Trans. parallel Distrib. Syst.*, vol. 22, no. 8, pp. 1249–1257, 2011.

[14] A. M. Patel and M. M. Patel, "A Survey of Energy Efficient Routing Protocols for Mobile Ad- hoc Networks," *Int. J. Eng. Res. Technol.*, vol. 1, no. 10, pp. 1–6, 2012.

[15] F. Corti, A. Reatti, L. Ciani, M. Kazimierczuk, A. Bartolini, and F. Grasso, "Analysis and Design of Stand-Alone Photovoltaic System for precision agricolture network of sensors," in *20th IEEE International Conference on Environment and Electrical Engineering*, 2020.

[16] R. Yan, H. Sun, and Y. Qian, "Energy-Aware Sensor Node Design With Its Application in Wireless Sensor Networks," *IEEE Trans. Instrum. Meas.*, vol. 62, no. 5, pp. 1183–1191, May 2013.

[17] M. T. Penella and M. Gasulla, "Runtime Extension of Low-Power Wireless Sensor Nodes Using Hybrid-Storage Units," *IEEE Trans. Instrum. Meas.*, vol. 59, no. 4, pp. 857–865, Apr. 2010.

[18] L. Gasparini, R. Manduchi, M. Gottardi, and D. Petri, "An Ultralow-Power Wireless Camera Node: Development and Performance Analysis," *IEEE Trans. Instrum. Meas.*, vol. 60, no. 12, pp. 3824–3832, Dec. 2011.

[19] L. Ciani, D. Galar, and G. Patrizi, "Improving context awareness reliability estimation for a wind turbine using an RBD model," in *2019 IEEE International Instrumentation and Measurement Technology Conference (I2MTC)*, 2019, pp. 1–6.

[20] D. Capriglione *et al.*, "Development of a test plan and a testbed for performance analysis of MEMS-based IMUs under vibration conditions," *Measurement*, vol. 158, p. 107734, Jul. 2020.

[21] D. Capriglione *et al.*, "Experimental analysis of IMU under vibration," in *16th IMEKO TC10 Conference 2019 - Testing, Diagnostics and Inspection as a Comprehensive Value Chain for Quality and Safety*, 2019.

[22] L. Ciani and G. Guidi, "Application and analysis of methods for the evaluation of failure rate distribution parameters for avionics components," *Measurement*, vol. 139, pp. 258–269, Jun. 2019.

[23] L. Ciani, A. Bartolini, G. Guidi, and G. Patrizi, "A hybrid tree sensor network for a condition monitoring system to optimise maintenance policy," *ACTA IMEKO*, vol. 9, no. 1, pp. 3–9, 2020.

[24] L. Ciani, A. Bartolini, G. Guidi, and G. Patrizi, "Condition Monitoring of Wind Farm based on Wireless Mesh Network," in *16th IMEKO TC10 Conference 2019 - Testing, Diagnostics and Inspection as a Comprehensive Value Chain for Quality and Safety*, 2019, pp. 39–44.

[25] M. Catelani, L. Ciani, A. Bartolini, G. Guidi, and G. Patrizi, "Characterization of a low-cost and low-power environmental monitoring system," in *2020 IEEE International Instrumentation and Measurement Technology Conference (I2MTC)*, 2020.

[26] D. Capriglione *et al.*, "Characterization of Inertial Measurement Units under Environmental Stress Screening," in *2020 IEEE International Instrumentation and Measurement Technology Conference (I2MTC)*, 2020.

[27] M. Catelani, L. Ciani, G. Guidi, and M. Venzi, "Parameter estimation methods for failure rate distributions," in *14th IMEKO TC10 Workshop on Technical Diagnostics 2016: New Perspectives in Measurements, Tools and Techniques for Systems Reliability, Maintainability and Safety*, 2016, pp. 441–445.

[28] M. Catelani, L. Ciani, G. Patrizi, and M. Venzi, "Reliability Allocation Procedures in Complex Redundant Systems," *IEEE Syst. J.*, vol. 12, no. 2, pp. 1182–1192, Jun. 2018.

[29] M. Catelani, L. Ciani, V. Luongo, and R. Singuaroli, "Evaluation of the Safe Failure Fraction for an electromechanical complex system: remarks about the standard IEC61508," in *2010 IEEE Instrumentation & Measurement Technology Conference Proceedings*, 2010, pp. 949–953.

[30] L. Ciani, G. Guidi, G. Patrizi, and M. Venzi, "System Maintainability Improvement using Allocation Procedures," in *2018 IEEE International Systems Engineering Symposium (ISSE)*, 2018, pp. 1–6.

[31] IEC 60068-2-14, "Environmental testing Part 2-14: tests - Test N: Change of temperature." International Electrotechnical Commission, 2011.

[32] IEST-RP-PR003.1, "HALT and HASS." Institute of Environmental Sciences and Technology - Product Reliability Division, 2012.

[33] MIL-STD-810G, "Environmental Engineering Considerations and Laboratory Tests," no. October. US Department of Defense, Washington DC, 2008.

[34] JEDEC Solid State Technology, "JEDEC STANDARD: Temperature cycling." JESD22-A104E, 2014.